Computation of Transition and Molecular Diffusivities in Fibrous Media

Rajesh R. Melkote
Dept. of Chemical Engineering and Materials Science, University of Minnesota, Minneapolis, MN 55455

Klavs F. Jensen
Dept. of Chemical Engineering, Massachusetts Institute of Technology, Cambridge, MA 02139

The tortuosities of fibrous media in the heretofore unexplored transition and ordinary regimes are computed using a Monte Carlo scheme based on the Einstein equation for random walkers. The model structure is that of fully penetrable cylinders (FPC) in a unit simulation volume. The mean square displacement technique is combined with the first passage time distribution to accelerate the progress of the walkers at low Knudsen number. The results include the computation of transition regime transport coefficients for the first time. The calculated ordinary tortuosities are approximately equal to the reciprocal of the porosity over a wide range, while the transition tortuosities are shown to deviate from the reciprocal porosity with a simple dependence on Knudsen number. The limits of the transition regime are shown to correspond roughly to Knudsen numbers of 0.50 and 100, respectively. The calculated Knudsen tortuosities are shown to improve on earlier results obtained by the authors using a flux-based technique.

Introduction

Transport through fibrous materials in the ordinary or continuum regime is a phenomenon pertinent to several physical problems of significance. Among these are diffusion in biological membranes, solute partitioning and transport in gels (Fanti and Glandt, 1989), and chemical vapor infiltration (CVI) of fibrous preforms (Naslain, 1986). CVI is seldom operated at high pressures, but the large pore sizes ($\sim 10^1 - 10^2\ \mu$m) imply that at least the transition regime is potentially pertinent even at moderate pressures. In a previous study (Melkote and Jensen, 1989) we have simulated the Knudsen regime diffusion in such structures, which dominates at the typically low pressures (<0.1 atm) and high temperatures ($\sim 1{,}000$°C). However, a thorough macroscopic description of the densification, wherein the average pore size decreases with time, requires a transport description (that is, diffusion and/or permeability) in the transition regime or molecular regime, especially if higher pressures are used, as in some of the newer variants of CVI. From this standpoint as well as a theoretical one, the effective molecular regime transport coefficients are of interest.

This problem is but a subset of the general topic of transport in disordered materials where the inhomogeneities are dispersed on a microscopic scale. Such problems have a long history which can be traced to Maxwell (1881) and Rayleigh (1892). A good review of the analytical methods as applied to these problems is given by Torquato (1987). The biggest drawback of such approaches is that they require extremely detailed microstructural information in the form of the nth-order correlation functions. For certain disordered materials, however, variational upper and lower bounds on the effective transport coefficient can be calculated; this has been done for random dispersions of interpenetrating spheres (Weissberg, 1963) and random dispersions of fully penetrable cylinders (FPC) (Tsai and Strieder, 1986). "Exact" solutions can be found where the correlation functions are known, as in regular arrays of cylinders (Keller, 1963; Perrins et al, 1979), or for certain computer-generated random arrays (Sangani and Yao, 1988), but these are exceptions. In all other cases, only bounds can

Current address of R. R. Melkote: Amoco Oil Company, P.O. Box 3011, Naperville, IL 60566.

be derived. The case of fiber-reinforced composites where the fiber placement is isotropic in the plane perpendicular to the generator of the fibers was dealt with by Beran and Silnutzer (1971). The famous Hashin-Shtrikman and Milton bounds have been evaluated for media composed of equal-sized cylinders in a matrix that are spatially uncorrelated (and thus allowed to overlap) (Torquato and Beasley, 1986), or impenetrable (Torquato and Lado, 1988), or possess an arbitrary degree of penetrability (Smith and Torquato, 1989). The first treatment of fully penetrable cylinders with random orientations in 2- and 3-D is due to Tsai and Strieder (1986), who derived bounds from a different variational principle, which requires formulation of a trial function for the field (temperature, electric,...). The resulting bounds should be useful in cases where the conductivities of the dispersed and continuous phases differ widely.

It is apparent that for arbitrary randomly disordered materials, the analytical methods are not directly useful, and hence explicit techniques must be used. Typically the latter involve the computational construction of a model of the disordered medium, and in the particular context of gas diffusion, the explicit simulation of the molecular pathways through the conducting (void) phase. In the pure Knudsen regime, this method involves the repeated calculation of paths from solid surface to solid surface, and has been successful (Evans et al., 1980; Burganos and Sotirchos, 1988; Melkote and Jensen, 1989). When the ratio of mean free path $\bar{\lambda}$ to mean pore dimension $\bar{d}$ begins to decrease, the proportion of intermolecular collisions increases relative to the number of molecule-solid interface collisions. The analysis then becomes somewhat more complex in the accounting of the collisions in the continuous (conducting) phase. Since an explicit molecular dynamics treatment is usually prohibitively expensive, a heuristic method is used wherein the path of the molecule is randomly perturbed after random time increments which are chosen according to some distribution which realistically represents the physics. This idea has been employed in the past (Abbasi et al., 1983; Akanni et al., 1987). The disadvantage of this step-by-step procedure is that if one is simulating low Knudsen numbers ($N_{Kn} \equiv \bar{\lambda}/\bar{d}$), a large number of such steps are required for a given molecule to traverse even the minimum distance necessary to adequately 'sample' the solid. Abbasi et al. (1983) recognized this and computed the distance increment Δx_j from an equation determined by piecewise linear regression of previous distance increments ($\Delta x_1, \ldots \Delta x_{j-1}$). While this is a faster means of advancing the molecules, it has the potential to introduce serial correlations. Akanni et al. (1987) did not use a pseudo-simulation and instead used explicit steps. There is good evidence, however, that an inadequate number of steps ($\sim 10^3$) was used and thus the tortuosity values they obtained do not accurately represent the solid. On the other hand, Schwartz and Banavar (1989) and Schwartz et al. (1989) used a similar random walk technique to measure electrical transport in various grain packings and found that $\sim 10^5$ steps are required to adequately explore the medium.

In the present work, we use a technique, suggested by Reyes and Iglesia (1991) and recently used by Tassopoulos and Rosner (1991), which retains some elements of the explicit step-by-step procedure. It is a hybrid method which moves the probing molecules rapidly through the continuum portions of the void space amid the dispersed phase, but reverts to a step-by-step method in a given neighborhood of the inclusions which constitute the dispersion. The gas transport through a fibrous medium, where the solid phase is represented as a dispersion of randomly located, interpenetrating, monodisperse, essentially infinite cylinders, is investigated under the transition and ordinary/molecular regimes. This medium is identical to the one subject to analyses by Tsai and Strieder (1986) and Faley and Strieder (1988b). The FPC medium is believed to be a good structural and transport model for the fibrous preforms during the course of CVI (cf. Melkote and Jensen, 1989, for further justification and geometric details). The ordinary regime results should be applicable to other transport processes in fibrous materials where the fiber phase is insulating, provided that the physical phenomena governing the transport occur on a length scale much smaller than that characteristic of the heterogeneities of the medium. To our knowledge this is the first such analysis for fibrous materials.

Theory/Technique

Background/equations

The calculation of effective molecular diffusivities in the FPC medium relies on the so-called mean square displacement (MSD) method. In dense gases, diffusion under the ordinary regime is analogous to Brownian motion. The instantaneous distribution of Brownian particles in one dimension is given by:

$$f(x,t) = \frac{n}{(4\pi Dt)^{1/2}} \exp\left(-\frac{x^2}{4Dt}\right) \tag{1}$$

where

$$n \equiv \int_{-\infty}^{\infty} f(x,t)dx. \tag{2}$$

If the medium through which diffusion is occurring is isotropic, the motions in each dimension are independent of one another and the mean square displacement in three dimensions is given by:

$$<S^2> = <x^2> + <y^2> + <z^2> = 6Dt \tag{3}$$

In the case of a two-phase composite medium where only the continuous phase occupying volume fraction ϕ conducts, Eq. 3 can be modified as

$$\phi <S^2> = 6D^{\text{eff}}t \tag{4}$$

where the diffusivity is now an effective value which incorporates the effects of periodic diffusion path interruptions caused by the dispersed phase (random walkers chosen in the solid phase automatically have $S^2 = 0$). Equation 4 is the basis for the simulations here. Recently, Tomadakis and Sotirchos (1991) have employed Eq. 4 to estimate Knudsen transport through randomly overlapping fibers.

The tortuosity factor commonly found in the engineering literature is defined as (Satterfield, 1970):

$$\tau \equiv \phi\left(\frac{D}{D^{\text{eff}}}\right) \tag{5}$$

The bulk diffusivity of a gas is given by kinetic theory as

$$D=\frac{1}{3}\bar{\lambda}\bar{v} \tag{6}$$

where $\bar{v}$ is the mean molecular velocity and $\bar{\lambda}$ is the mean free path of the gas under the diffusion conditions. Combination of Eqs. 4-6 yields

$$<S^2>=\left(\frac{2\bar{\lambda}\bar{v}}{\tau}\right)t \tag{7}$$

Eq. 7 suggests a simulation method wherein if random walkers (representing individual molecules) are allowed to probe the porous medium for the same fixed time interval t_o, a plot of $<S^2>$ vs. t should be linear and the slope should yield a measure of the tortuosity of the structure. The success of the scheme depends, of course, on whether accurate $<S^2>$ data can be generated for each particle in accordance with the physics of the problem, which includes collisions with other particles and with the solid surfaces which comprise the interfacial area of the disordered composite. If one assumes purely hard sphere-type collisions, so that the movements of a given particle after different intervals of time are mutually independent processes (Einstein, 1926), a random walk with no memory in a three-dimensional continuum can be a reasonable approximation to the actual motion of the diffusing particle.

The probe time t_o must be sufficiently long so as to adequately explore the structure, so that the computed τ represents the actual tortuosity of the medium. Typically this requires that displacements of a few pore dimensions be traversed (this will be made more precise later). Since N_{Kn} ($\equiv\bar{\lambda}/\bar{d}$) is by definition small in the molecular regime, and a typical molecular step is of the order of $\bar{\lambda}$, a very large number of steps may be required for each walker. In fact, if a molecule must traverse a net displacement of $N\bar{d}$ to adequately probe at a Knudsen number of 10^{-2}, from Eq. 7 the average number of individual steps required is

$$n=\frac{\tau}{2}N^2\left(\frac{\bar{d}}{\bar{\lambda}}\right)^2\sim N^2 10^4 \tag{8}$$

or on the order of 10^5, depending on the porosity, as found by Schwartz and Banavar (1989). In the present analysis, we opt for a more elegant scheme that allows a walker to take large steps (each of which is equivalent to several small steps of the order of $\bar{\lambda}$) when it is sufficiently far from a solid surface (pseudo-continuum regime), and take smaller steps in the vicinity of a solid surface (discrete regime). This hybrid scheme has been suggested by Reyes and Iglesia (1991) in the context of transport in sintered sphere assemblages and will be outlined next.

The first passage time (FPT) distribution of interest is the probability $P(t,x=0;R)$ for a travel time t for a particle starting from the center of a sphere of radius R and reaching the surface of the sphere for the first time, given as:

$$P(t,x=0;R)=1+2\sum_{n=1}^{\infty}(-1)^n\exp\left(-\frac{Dn^2\pi^2 t}{R^2}\right) \tag{9}$$

References to the derivation of Eq. 9 can be found in Weiss (1967). This is a useful result because it implies that since the probability density of first passage times is known, the diffusing molecule can be advanced by a single step R_i, which is equivalent to arriving at the same point by a zigzag path composed of several segments of the order of $\bar{\lambda}$, in time t_i. The compilation of S^2 vs. t data for Eq. 7 is accelerated precisely because the steps R_i are much larger than $\bar{\lambda}$; furthermore, the solution (Eq. 9) is strictly valid only for $R_i \gg \bar{\lambda}$. The exploitation of the FPT in the context of exploring fibrous media is explained in the next section.

Simulation procedure

Generation of Model Fibrous Medium. The diffusion simulations are all performed on the fully penetrable cylinders (FPC) construction, purported to be a representation of a fibrous medium. The cylinders are generated by choosing N_c random points in a cubic volume and assigning direction cosines to them at random, thus defining the cylinder axes. Based on the desired porosity ϕ the radius of the cylinders is chosen by

$$r_f=\left[\frac{-\ln\phi}{\pi N_c\left(\sum_i l_{f_i}/N_c V\right)}\right]^{\frac{1}{2}} \tag{10}$$

where l_{f_i} are the axis lengths and V is the volume of the cube, set to unity (thus normalizing r_f and l_{f_i} by the edge length). Thus the locations and orientations of the cylinders are completely uncorrelated. The axes are effectively truncated at the cube faces so that a distribution of l_{f_i} results. Since points within the cube are chosen and used to generate the cylinders for computational convenience, the properties of the structure may differ slightly from those of a true 3-D cross-section of randomly oriented infinite cylinders in space. For cylinders generated in this manner in a unit cube (I-randomness in the terminology of Coleman (1969)), it has been shown that the average axis length can be calculated exactly:

$$\sum_i l_{f_i}/N_c=1+\frac{1}{\pi}\ln 2+\left(\frac{3}{2}-\frac{5}{4\pi}\right)\ln 3-\frac{4\sqrt{2}}{\pi}\tan^{-1}(1/\sqrt{2})$$
$$-\frac{6}{\pi}\int_0^1\frac{\tan^{-1}w}{w+2}\,dw=0.896 \tag{11}$$

The average secant length in all of our computed structures was nearly identical to this value. N_c is chosen to be sufficiently large that a test particle in a typical void region perceives that it is in a dispersion of infinitely long fibers. This supposition will be accurate if very few or none of the test particles venture near a cube face (that is, the boundary of the simulation volume). This is less likely to be true for structures with high open porosity, especially if the free paths of the particles are large relative to the mean pore dimension, and thus some degree of anisotropy will exist near the cube faces. The mean pore dimension in the generated structure is given by the engineering formula

$$\bar{d}=\frac{4\phi}{s}=\frac{2}{\pi r_f N_c\left(\sum_i l_{f_i}/N_c V\right)} \tag{12}$$

where s is the interfacial surface area per volume of the dispersion. Further details of the generation and resulting geometry of the FPC are given by Melkote and Jensen (1989).

Molecular Travel. We now present the algorithm for the diffusion simulation using the mean square displacement method. The novelty of the procedure lies in the use of the FPT to advance molecules more rapidly through the pore space of the fibrous medium. The initial location of a walker (test molecule) is chosen at random and this origin is preserved. A search is performed to locate the nearest cylinder surface to this point, and an imaginary sphere is constructed centered at this point so that it is just tangent to the closest cylinder surface. The radius of the sphere, R_i, is just the distance to the surface (Figure 1). A point is chosen at random on the surface of this imaginary sphere, and the molecule is advanced by a distance R_i to this point. The search procedure is repeated to locate the closest solid surface to this point, another imaginary sphere is constructed, and so on. As noted earlier, if the radius of this sphere is of the same order as the mean free path $\bar{\lambda}$, use of this procedure is invalid. In fact, this procedure does not properly account for the dynamics of a molecule-wall collision and subsequent rebound (except in the limit $N_{Kn}=0$, where it is rigorously valid), since the probability of randomly choosing the exact tangency point is zero. Secondly, if a particle has reached a solid surface (within some tolerance ϵ) some type of scattering must be introduced for it to continue its journey. Reyes and Iglesia (1991) used this imaginary sphere construction method in the simulation of diffusion in sintered sphere assemblages. The wall collision mechanism is introduced here by switching to a step-by-step 'discrete' simulation when the imaginary sphere method brings a particle to within some small distance δ of the surface. This is equivalent to considering each cylinder to be surrounded by a boundary layer of thickness δ. The rudiments of this scheme are illustrated in Figure 1. Upon entering this layer, usually a few mean free paths thick, the particle is assigned direction cosines at random. A search is then performed to calculate the distance to the nearest cylinder surface that lies in the particle's trajectory. This distance is then compared to a random variate λ taken from the exponential distribution which characterizes molecular mean free paths (Loeb, 1934):

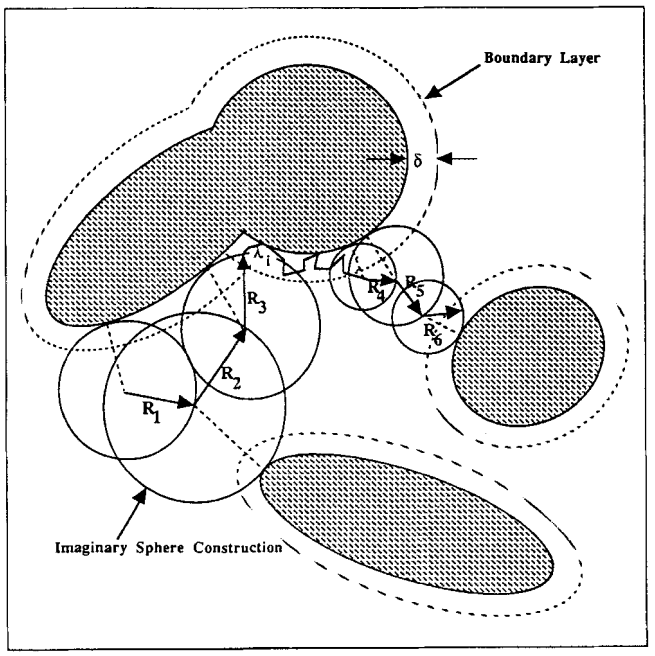

Figure 1. First passage time/discrete technique.

$$f(\lambda)=\frac{1}{\bar{\lambda}}e^{-\lambda/\bar{\lambda}} \tag{13}$$

using the equation

$$\lambda=-\bar{\lambda}\ln\xi$$

$$\xi \text{ uniform } \epsilon\ (0,1) \tag{14}$$

The molecule is advanced by the smaller of the two distances. If a wall collision occurs, the particle undergoes diffuse scattering and its direction cosines are modified accordingly (see Melkote and Jensen, 1989, for pertinent equations). When this step-by-step advance eventually brings the molecule out of the boundary layer, the FPT/imaginary sphere 'continuum' method is resumed. The tracer travel is continued until the desired probe time t_o is reached.

In terms of the above hybrid scheme, S^2 and t for Eq. 7 can be calculated for the continuum and discrete regimes. The square displacement is simply the square of the instantaneous distance from the initial starting point:

$$S^2=(x-x_o)^2+(y-y_o)^2+(z-z_o)^2 \tag{15}$$

As a measure of time, Eq. 7 suggests that the actual distance $\bar{v}t$ can be equivalently used:

$$\bar{v}t=\bar{v}t_{\text{cont}}+\bar{v}t_{\text{disc}} \tag{16}$$

To obtain t_{cont}, which should be a sum of variates from the FPT distribution, a dimensionless form of Eq. 9 is convenient:

$$P(t')=1+\sum_{n=1}^{\infty}(-1)^n\exp(-n^2\pi^2t') \tag{17}$$

where $t'\equiv Dt/R^2$. Then using Eq. 6,

$$\bar{v}t_{\text{cont}}=\bar{v}\sum_i t_i=\bar{v}\sum_i R_i^2t_i'/D=3\sum_i R_i^2t_i'/\bar{\lambda}. \tag{18}$$

Equation 18 can be simplified further if, for repeated use of the imaginary sphere construction, we can approximate:

$$\sum_i R_i^2t_i'\approx\overline{t'}\sum_i R_i^2 \tag{19}$$

$\overline{t'}$ is simply:

$$\overline{t'}=\int_0^{\infty}t'\frac{\partial P}{\partial t}(t')dt'=\frac{1}{6}. \tag{20}$$

Use of the mean passage time $\overline{t'}$ instead of computing a variate from Eq. 17 has been shown to save much computer time (Torquato and Kim, 1989). $\bar{v}t$ can then be written as

$$\bar{v}t = \sum_i R_i^2/2\bar{\lambda} + \sum_j \lambda_j \tag{21}$$

where λ_j are free paths in the discrete regime as chosen from the exponential distribution Eq. 13 or a search over cylinder surfaces. During the simulation, S^2 vs. $\bar{v}t$ data are averaged over several random walkers, and the slope of the resulting linear plot yields the tortuosity:

$$\tau = \frac{2\bar{\lambda}}{(\text{slope})} \tag{22}$$

In the ordinary regime, $\bar{\lambda}$ in the solid and free space are substantially the same. Note that for simulations in the transition and Knudsen regimes, $\bar{\lambda}$ must be replaced by the true mean free path, which is ϵ $(\bar{\lambda}, \bar{d})$. Figure 2 shows some typical $\overline{S^2}$ vs. $\bar{v}t$ plots at several Knudsen numbers. Of note is the fact that at small N_{Kn} the total travel distance required to achieve the same net displacement is much greater due to the larger number of erratic, zigzag path lengths (most of which are not actually traversed by virtue of the FPT method). Note that the actual distance travelled is often several multiples of the simulation cell edge length. Finally, the termination criterion for a particular walker can be expressed in terms of when the probe distance roughly equals N pore dimensions:

$$(\bar{v}t)_{\max} \approx \frac{(N\bar{d})^2}{2\bar{\lambda}}\,\tau \tag{23}$$

It should be noted that since τ is a priori unknown, the calculation of $(\bar{v}t)_{\max}$ is approximate. Finally, in this time interval, there will be a distribution of squared pore distances S^2, whose mean is desired to be $(N\bar{d})^2$. Typical distributions of probe distances, corresponding to the simulations in Figure 2, are illustrated in Figure 3. Note that the distribution is nearly invariant with N_{Kn} and resembles a Rayleigh-type density. The fact that this distribution is wide further emphasizes the notion that diffusion is an aggregate phenomenon; while individual molecules may attain varying displacements, their density (Eq. 1) obeys the diffusion equation.

It should be noted that spherical enclosures are used in the FPT/continuum procedure merely for convenience, since cylindrical surfaces are similarly convex. For other dispersions, different enclosure geometries may be more natural; however, the diffusion equation has to be re-solved for the FPT accordingly. In their simulation of Brownian motion in various 2-D constricted pore arrangements, Siegel and Langer (1986) used box-shaped enclosures to advance the walkers. They also derived the FPT result for circular enclosures, which may be of more general utility in 2-D problems.

Results and Discussion

In this section we present results for the tortuosities of the FPC structures computed from the technique previously described. Before doing so, some details common to all of the cases must be provided.

The model structure used is an FPC dispersion in a unit cube. To avoid correlations of any kind, periodic boundary conditions are not employed. Instead, the sample size (as quantified by the number of cylinders in the volume, N_c) is made as large as necessary. The boundary conditions become an issue only if walkers stray near a boundary and/or collide with it. Thus N_c has to be increased (thus reducing the cylinder radius for a given porosity) as much as practicable to minimize the number which reach a boundary (that is, escape). While the avoidance of boundary conditions is elegant, it is not practical at high porosities due to the large N_c required to maintain a low escape percentage. The drawback is that time is added to the search procedure which is performed frequently. There-

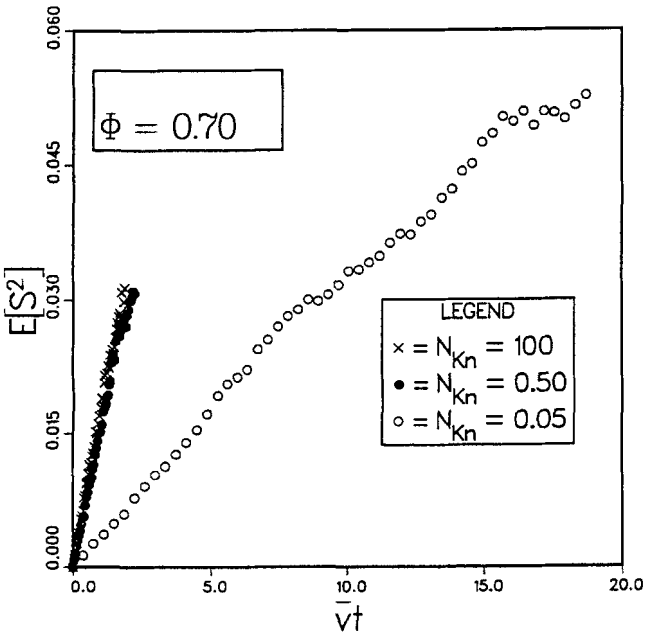

Figure 2. Typical $\bar{S}^2$ vs. $\bar{v}t$ plots, showing linearity.

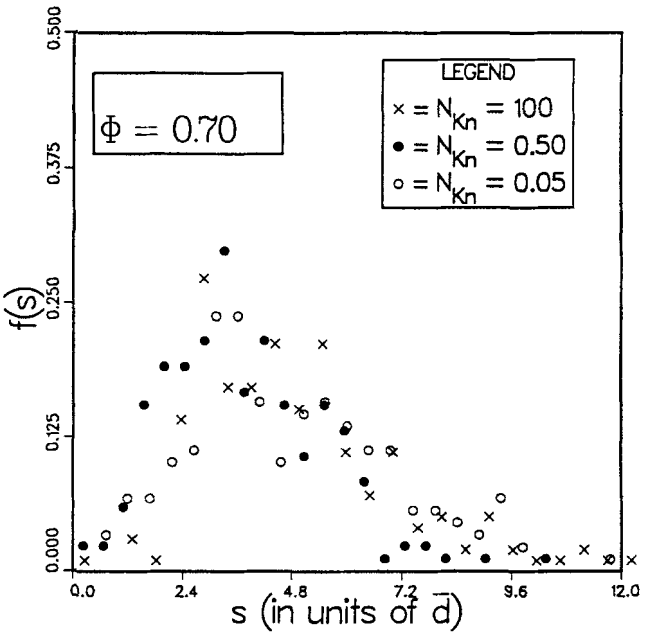

Figure 3. Typical distribution functions of particle net displacement.

fore, the further precaution is taken of choosing the origins of the walkers only in a certain radius of the center of the cube, which will depend on the required probe distance (see Figure 4). In the current analysis, for instance, $N_c \approx 1{,}400$ was sufficient to reduce the escape fraction to $\leq 5\%$ in the ordinary regime for $\phi \leq 0.5$ and a probe distance of nearly $6\bar{d}$. Moreover, the connectivity of the structure decreases at low ϕ due to percolative effects, so that the escape fraction naturally declines for a given N_c. At higher porosities, due to higher connectedness a larger fraction escapes. $N_c \approx 1{,}500$–$1{,}800$ was required in these cases. Note that the practice of initiating the walkers only in a smaller region about the cube center does introduce some bias into the diffusivity calculation, but by averaging the results over several realizations (different structures with the same ϕ) this bias is minimized.

The number of mean pore dimensions ($N\bar{d}$) required to probe adequately needs to be determined also. While it is obvious that $N_{\min} > 1$, the actual N has to be determined by experimentation. We found that 5–6 mean pore dimensions need to be traversed before a reliable tortuosity value is obtained which is not sensitive to further probing. This probe distance is required for correlation coefficients of 0.99 or greater to be obtained in the linear regression of S^2 vs. $\bar{v}t$, especially in the transition and Knudsen regimes. When only $0.5\bar{d}$ or so is explored, the tortuosity is roughly unity, that is, the molecule is oblivious to the fact that it is inside a two-phase material. In the ordinary diffusion simulations of Akanni et al. (1987) who used the step-by-step method, Eq. 8 can be used to show that in their random sphere dispersions, only 0.39–$0.55\bar{d}$ were probed in the "cannonball" solids, and only 0.27–$0.42\bar{d}$ were probed in the "Swiss cheese" solids. Their results are thus insensitive to the nature of the pore walls (convex or concave) as well as nearly invariant with ϕ, a clearly unphysical result.

Finally, there is the question of how many walkers to include in the computation of $E[S^2]$. This was determined by plotting the calculated τ vs. N_M, the number of walkers and judging when the fluctuations become sufficiently small. $N_M = 200$ was used in all cases. To obtain the mean and standard error of τ, the results were obtained from ten different realizations of the medium at each porosity investigated.

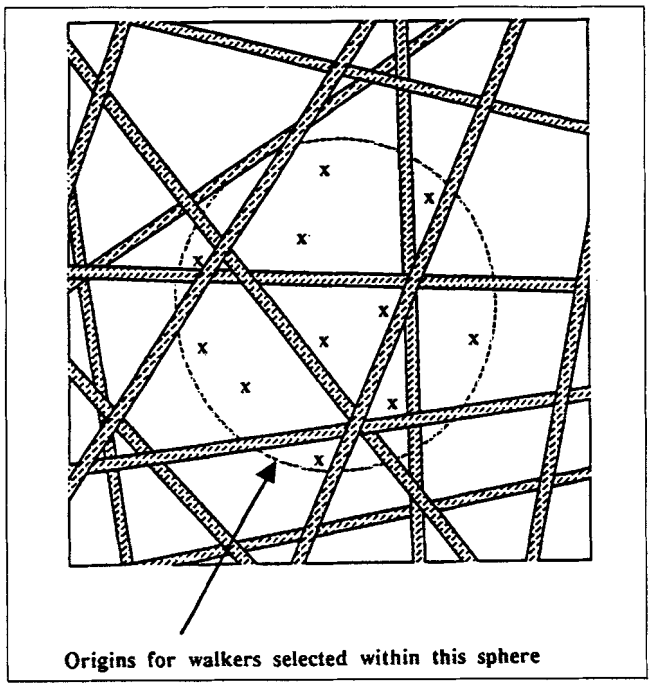

Figure 4. Simulation volume, showing selection of starting points for random walkers.

Ordinary Regime

Computational issues

The main adjustable computational parameter here is δ, the boundary layer thickness. The tortuosity results at one porosity value are shown in Table 1. As mentioned earlier, δ should be on the order of a few mean free paths; here we have shown the effect of δ on the computed τ. The effect appears to be negligible for δ from $2\bar{\lambda}$ to $7\bar{\lambda}$. Our choice of δ is thus dictated by other factors. At higher δ, the amount of time spent in the discrete regime is greater, while at lower δ, the amount of overhead associated with the increased frequency of entries/exits from the boundary layer increases. A moderate value of $\delta = 5\bar{\lambda}$ was chosen which appears to give negligibly different tortuosities at lowest computational cost. Of course $\delta = 0$ cannot be used because the particle becomes 'trapped' at the cylinder surface. Furthermore, there is a natural upper limit:

$$\frac{\delta}{\bar{\lambda}} \leq \frac{1}{2N_{Kn}} \tag{24}$$

Therefore for $N_{Kn} \geq 0.5$, in the transition regime, we are forced to use a pure discrete simulation. To further minimize the expense associated with the discrete procedure in the ordinary regime, the repeated searches at each step are performed only over nearest neighbor cylinders within an inclusion distance d_{inc} (Verlet, 1968). These Verlet lists are updated as infrequently as possible; the optimal frequency was found to be whenever the distance d that has been covered since the last update satisfies

$$\frac{d}{d_{\text{inc}}} \geq 1 - 4N_{Kn}\left(\frac{\bar{d}}{d_{\text{inc}}}\right) \tag{25}$$

which essentially assumes that there is a low probability of a variate $\lambda_j \geq 4\bar{\lambda}$ being generated by the exponential distribution (Eq. 13). In the ordinary regime $d_{\text{inc}} = \bar{d}$ sufficed in all cases.

Results

In Figure 5, we present tortuosities in the ordinary regime at several porosities and Knudsen numbers of 0.05 and 0.025. That these N_{Kn} values very nearly represent the molecular re-

Table 1. Effect of Boundary Layer Thickness

$\delta/\bar{\lambda}$	τ ($\phi = 0.70$, $N_{Kn} = 0.05$)	CPU sec/traj (Cray-2)
2	1.42	2.37
4	1.37	1.19
5	1.46	1.01
6	1.40	1.05
7	1.42	1.04

gime asymptote is revealed by the ratios of the actual mean free path in the solid ($\bar{\lambda}_{true}$) to that in free space ($\bar{\lambda}_{free\ space}$). At $N_{Kn}=0.05$ and 0.025, $\bar{\lambda}_{true}/\bar{\lambda}_{free space}=0.93$ and 0.97 respectively. A plot such as Figure 8 (to be discussed in the next section) can be used to verify this also. The error bars represent one standard deviation (σ) based on ten realizations. Shown for comparison are several variational bounds and/or approximate expressions. The solid line is the famous Hashin-Shtrikman (1962) bound, $\tau \geq 1+(1/2)(1-\phi)$, which is the best bound for an arbitrary two-phase dispersion if only the void fraction and individual phase conductivities are known. The variational bound of Weissberg (1963), $\tau \geq 1-(1/2)\ln\phi$, was derived for a bed of randomly overlapping monodisperse spheres and is an improvement over the H-S bound due to the inclusion of this additional microstructural information. The best available bound for the FPC medium is that of Tsai and Strieder (1986) and is given by $\tau \geq 1-(2/3)\ln\phi$. This bound is derived assuming local diversion of the flux so as to negotiate the irregular paths around insulating fibers and is expected to be a good estimate of the conductivity at high bed dilution. Our simulation results tend toward this bound at high porosities. Tsai and Strieder report an experimental τ value by Penman of 1.51 for $\phi=0.691$; our calculated value at $\phi=0.70$ is $\tau=1.46\pm0.050$. Finally, the expression of Wakao and Smith (1962), $\tau=1/\phi$, which was obtained as the bulk diffusion limit for transport in macropore-micropore systems, is shown to be a good approximation to the simulation results. Deviations are noted at lower porosities. While this agreement is fortuitous in the sense that the porosity ϕ has been divided out of Eq. 7, it implies that in the ordinary limit the diffusion mechanism through the FPC resembles that in a simplified macropore-micropore assemblage.

Kim and Torquato (1990) recently simulated effective (transverse) conductivities in equilibrium distributions of infinitely long, oriented hard (that is, insulating) cylinders using a variation of the technique here. Instead of explicit steps in the boundary layer, they derived the mean hitting times and probabilities for a particle in a small neighborhood of the interface. The results for a few cylinder volume fractions (from their Figure 11) are compared with the present simulations for $N_{Kn}=0.025$ in Table 2. Interestingly, the agreement is very good.

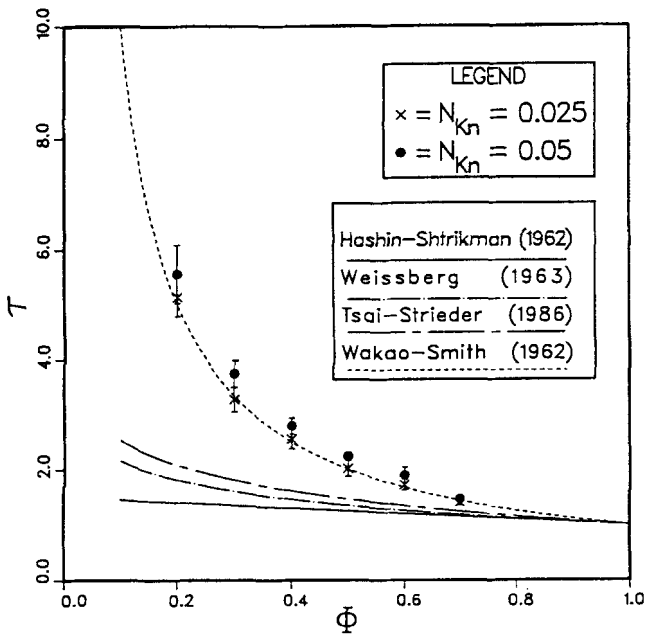

Figure 5. Ordinary regime tortuosities and comparisons with bounds.

At lower porosities ($\phi \leq 0.30$), we note a greater deviation from this simplified picture and an increase in the standard deviation of τ. Both observations are related to the existence of disjoint void clusters at high fiber concentration. This was observed in our ϕ^A simulations for total porosities less than ≈ 0.42 (Melkote and Jensen, 1989) but has been observed at much lower porosities by Tomadakis and Sotirchos (1991). As a consequence of this percolative behavior, the walkers may explore different regions of the void space which may not be connected to one another and which may have significantly different transport characteristics. The connections which do exist are likely to be narrow necks due to the convex nature of the inclusions. Therefore we would expect large fluctuations in the tortuosity calculated by this method as the porosity decreases, particularly as the percolation threshold ϕ_c (≈ 0.095) is approached.

Transition and Knudsen regimes

In this section we extend the analysis using the mean square displacement (MDS) method to the heretofore unexplored transition regime and the Knudsen regime which was previously studied. Again, the computational issues are discussed first.

Computational Issues. In the transition and Knudsen regimes, the hybrid FPT technique is no longer profitable, since the thickness of the largest boundary layer that can be constructed is less than or equal to a typical free path length (see Eq. 24). Therefore, a pure discrete simulation is used, which is expensive at low $\bar{\lambda}$ and is cheapest at the Knudsen limit. In this simulation, a comparison is made at each step between a free path (from Eq. 13) and the distance to the nearest cylinder surface along the trajectory line, and the particle is advanced by the smaller distance. Due to the greater overhead involved in performing this search much more often, we would expect the computations to be more expensive. A timing comparison between the hybrid FPT and discrete techniques is made at $N_{Kn}=0.50$, which is probably the upper limit at which the former can be used, and is presented in Table 3.

First, the quantitative results for τ via the two methods agree very well, yielding some confidence in the use of the hybrid technique in the ordinary regime. Second, the hybrid technique does save much time even though the inclusion distance d_{inc} has been increased from $\bar{d}$ to $4\bar{d}$ due to the higher N_{Kn}. Computation times are reduced by an order of magnitude on the average, and this saving would only increase at lower N_{Kn}, since the number of discrete steps $n \sim N_{Kn}^{-2}$ (see Eq. 8).

In general, larger sample sizes were required for higher N_{Kn}, since the fraction of particles escaping from the simulation

Table 2. Comparison of D^{eff}/D at $N_{Kn}=0.025$

Cylinder fraction $(1-\phi)$	Kim & Torquato (1990) (Figure 11)	Present Simulations
0.30	0.508	0.500
0.50	0.279	0.249
0.70	0.121	0.092

Table 3. Comparison of MSD w/ and w/o FPT

ϕ	τ at $N_{Kn}=0.50$		CPU sec/traj (Cray-XMP)	
	Hybrid	Discrete	Hybrid	Discrete
0.20	5.61±0.350	6.14±0.500	0.22	3.05
0.30	3.91±0.170	3.83±0.166	0.18	1.73
0.40	2.80±0.132	2.77±0.114	0.15	1.21
0.50	2.30±0.169	2.35±0.128	0.17	1.10
0.60	1.90±0.137	2.05±0.151	0.18	1.00

volume increased for the same probe distance. Furthermore, the required sample size using this technique increases rapidly with porosity at high ϕ, since $N_c \sim (-\ln \phi)^{-1}$. For instance, $N_c \approx 2{,}200$ was required for pure Knudsen simulations at $\phi = 0.70$, while $N_c \approx 5{,}400$ was required at $\phi = 0.80$ to maintain the low escape percentage. The use of some type of boundary condition thus becomes essential at such high porosities. It is difficult to impose truly periodic boundary conditions on a random fiber unit cell which is intrinsically nonperiodic, and some approximation such as specularity must be used.

At this point, it should be emphasized that the main drawback of the MSD technique, as with most particle simulation methods, is the large computational requirement. However, since the particle histories are essentially independent of each other, a parallel machine could be used to obtain results at a rate suitable for experimentation and parameter studies. [This computational decoupling has been achieved even in the ordinary and transition regimes by use of the free path distribution, Eq. 13]. Furthermore, the memory requirements are small (<1 MW) so that small samples may be investigated on a high speed workstation.

Results

In the transition regime, the number of wall collisions is comparable to the number of intermolecular collisions, and thus the inclusion geometry would be expected to be more influential than in the ordinary limit. The toruosities are expected to be higher because of an increasing number of path reversals forced by the diffuse scattering at the walls. This is indeed evidenced by the data at $N_{Kn} = 0.50$ and $N_{Kn} = 1.0$ shown in Figure 6, which now deviate strongly from $\tau = 1/\phi$. It is important to note that the tortuosities in Figure 6 were calculated using the true mean free path, that is, the actual distance between collisions as obtained during a simulation, in the bulk diffusivity (see Eq. 6). While this did not differ significantly from the free space value ($\bar{\lambda}_{free} \equiv N_{Kn}\bar{d}$) in the ordinary regime, it does differ in the transition and Knudsen regimes as the wall effects become stronger. For instance, at $N_{Kn} = 0.50$, $\bar{\lambda}_{true}/\bar{\lambda}_{free\ space} = 0.62$, and at $N_{Kn} = 1.0$, $\bar{\lambda}_{true}/\bar{\lambda}_{free} = 0.43$. When this ratio is accounted for in calculating a τ based on the free space value of $\bar{\lambda}$, the result is as shown in Figure 7, where the ordinary regime values are included for comparison. One would expect a τ defined in this manner to increase monotonically with N_{Kn}, since $\bar{\lambda}_{free} \alpha N_{Kn}$ but $\bar{\lambda}_{true} \to \bar{d}$. The τ of Figure 7 may be more useful in practical problems where the $\bar{\lambda}_{free}$ can be calculated from the temperature and pressure but $\bar{\lambda}_{true}$ is unknown *a priori*. Thus the Knudsen numbers discussed in this study refer to the nominal values based on $\bar{\lambda}_{free}$. From a theoretical standpoint, however, the

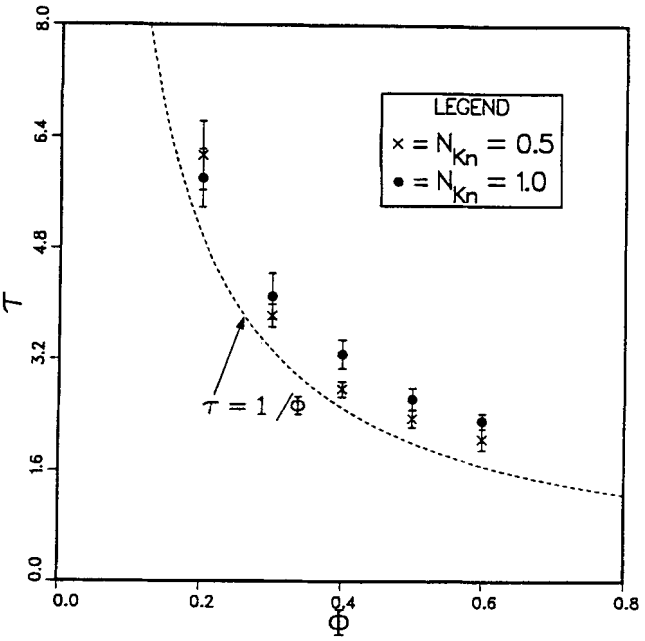

Figure 6. Transition regime tortuosities.

tortuosities in Figure 6 are truly representative of the obstructionism of the porous medium.

The tortuosities based on the true mean free path were computed for several more Knudsen numbers (at fixed porosity) and the results are shown in Figure 8. This plot is useful in precise determination of the limits of the transition regime. It is evident that the lower molecular asymptote is reached for $N_{Kn} \leq \sim 10^{-1}$ while the Knudsen asymptote is reached when $N_{Kn} \geq \sim 10^{2}$. Thus the transition regime can be defined for $N_{Kn} \in (0.5, 100)$ where τ increases proportionally with $\log N_{Kn}$. This type of delineation has not been performed, to our knowledge, for diffusion in fibrous media. Tassopoulos and Rosner (1991) found a very similar relationship between toruosity and Knudsen number in their anisotropic particulate systems, while

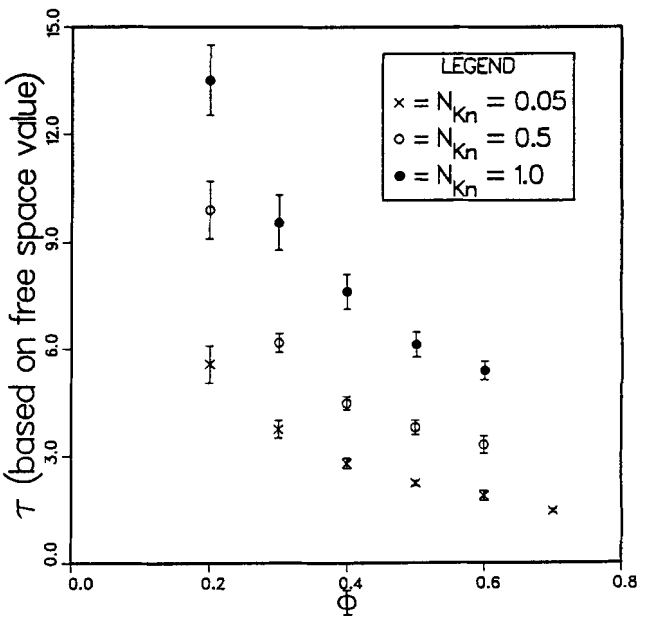

Figure 7. Tortuosities normalized by $\bar{\lambda}_{free}$.

Reyes and Iglesia (1991) found the tortuosities at the extremes of Knudsen number to be approximately equal. The latter suggests the existence of an appropriate pore length scale, based on which the tortuosities are independent of the diffusion regime. While a definition based on such a length scale is obviously desirable, it is impossible to determine this scale *a priori* for a given geometry.

Figure 8 suggests that perhaps a simple relationship can be suggested to correlate tortuosities in the transition regime with porosity and Knudsen number. The data at $\phi = 0.40$ and $N_{Kn} \in [0.50, 100]$ were fit to an equation of the form

$$\tau - \frac{1}{\phi} = a + b \ln N_{Kn} + c(\ln N_{Kn})^2 \tag{26}$$

The tortuosities according to Eq. 26 were then compared to computed values at several Knudsen numbers in this range; this is shown in Figure 9 for $0.20 \leq \phi \leq 0.60$. This simple equation works well except at the lowest porosity value. A general correlation with a more exact ϕ dependence could be obtained by nonlinear regression on a larger data set. A comparison can also be made with the oft-used Bosanquet relation for mixed diffusion in a straight capillary (Aris, 1975). It can be readily shown that

$$\frac{D^{\text{eff}}}{D_{\text{Bosanquet}}} = \frac{\phi}{\tau} \frac{\bar{\lambda}_{\text{true}}}{\bar{\lambda}_{\text{free}}} (1 + N_{Kn}) \tag{27}$$

This ratio is 0.93 ϕ/τ at $N_{Kn} = 0.50$ and 0.86 ϕ/τ at $N_{Kn} = 1.0$.

It is interesting to compare the Knudsen limit tortuosities obtained using the present MSD technique with those previously obtained using the $f_T - L$ (transmission probability) technique. Since at the Knudsen limit $\bar{\lambda}_{\text{true}} \approx \bar{d}$, the results of Figure 8 in Melkote and Jensen (1989) were converted to tortuosities and were plotted (without their error bars, for clarity) in Figure 10 using the definition:

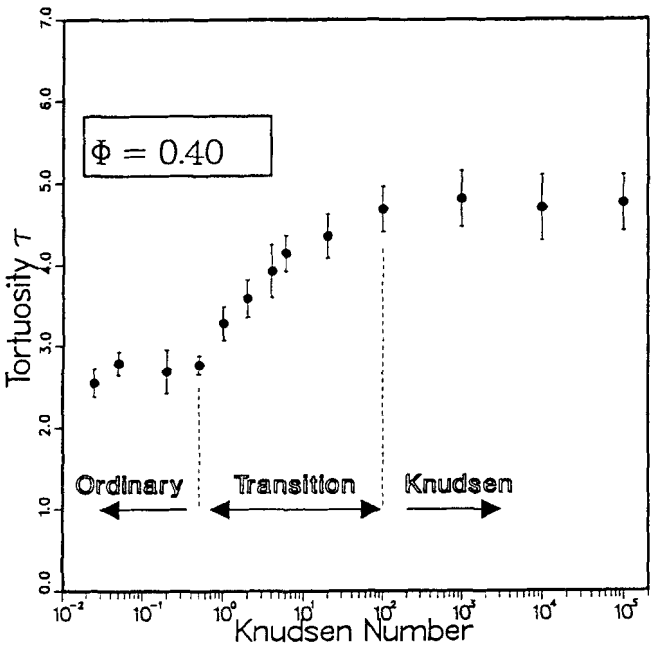

Figure 8. Tortuosity variation with Knudsen number.

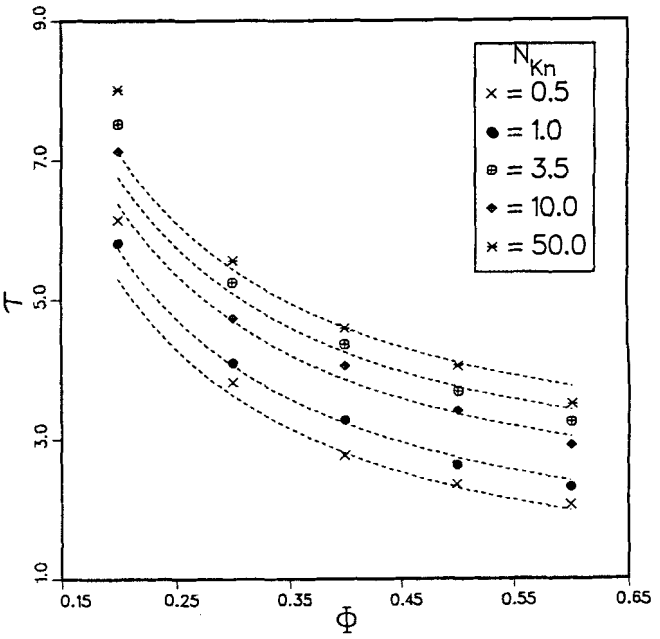

Figure 9. Comparison of simple equation fit (equation lines) with transition regime tortuosities.

$$\tau_{Kn} \equiv \phi \left(\frac{D(\bar{d})}{D^{\text{eff}}} \right) \tag{28}$$

Included are the new calculations of τ_{Kn} at $N_{Kn} = 100$ with $\pm \sigma$ error bars. It is apparent that the two methods agree remarkably well. This may seem surprising if one considers that the old transmission probability technique employed an elongated cell with fewer cylinders, used periodic boundary conditions in two dimensions, and only made use of x-direction displacement data. These 'shortcomings' appear to be reflected only in the greater amount of scatter in the previous data, while the quantitative agreement is likely due to the fact that an adequate number of pore dimensions were explored in the old technique by the requirement that a sufficient number of molecules penetrate to a depth of 1/3 of the cell length or more to obtain good linearity in f_T vs. $1/L$. It should be noted that even small escape fractions, on the order of 5 percent, can contribute to large percentage errors in the computed tortuosity. It can be shown using Eq. 1 that the errors in the zeroth moment and second moment, representing the escape fraction and error in the mean square displacement respectively, can be given approximately by

$$e_0 = 1 - \frac{1}{2\sqrt{\pi}} \int_0^{\xi} \exp(-\eta^2/4)\eta^2 \, d\eta \tag{29}$$

$$e_2 = 1 - \frac{1}{12\sqrt{\pi}} \int_0^{\xi} \exp(-\eta^2/4)\eta^4 \, d\eta \tag{30}$$

where e_0 as $e_2 \to 0$ as $\xi \to \infty$, and ξ is a normalized measure of the dimension of the simulation volume. Since application

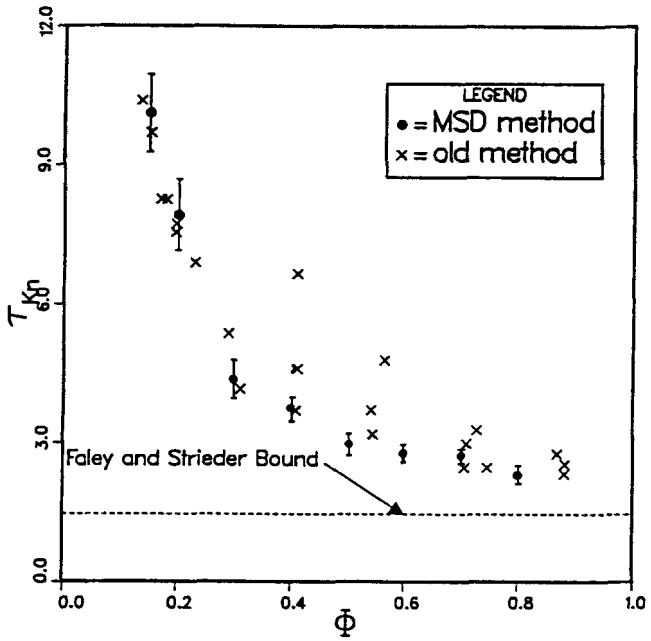

Figure 10. Comparison of Knudsen tortuosities computed by present (MSD) technique and old (transmission probability) method.

of Eqs. 29 and 30 showed that escape fractions of 5–6 percent resulted in ≈ 19 percent error in tortuosity,

$$\tau_{\text{actual}} = \tau_{\text{calculated}}\,(1 - e_2) \tag{31}$$

the Knudsen tortuosities in Figure 10 were subsequently adjusted downward.

Also shown in Figure 10 is the variational upper bound on the Knudsen tortuosity due to Faley and Strieder (1988),

$$\tau_{Kn} \geq \frac{13}{9} \tag{32}$$

While porosities exceeding 0.80 were not investigated due to prohibitive sample sizes, it is expected that this bound should be reached asymptotically as $\phi \rightarrow 1$. Note once again the increasing magnitude of the error bars with decreasing porosity in Figure 10, which is a consequence of the isolated cluster formation. At high porosities where the pore space is highly connected the standard deviation among multiple realizations is small. This notion is related to the "smooth field" assumption (Jackson, 1977) which is necessary to be able to formulate the continuum equations in a disordered porous medium. Based on our observations of the magnitude of the scatter in τ, it appears that only for the critical region $\phi_c < \phi < 0.20$ are the smooth field conditions in question. In CVI, this is normally only a concern over a small duration of the densification and is often ignored when formulating a process description. However, it should be kept in mind while interpreting results obtained from a macroscopic model of the process.

Conclusions

In this study, we have extended the study of effective diffusivities in fibrous media to include the spectrum of Knudsen numbers from the ordinary (molecular) regime to the Knudsen limit. The mean square displacement (MSD) technique based on Brownian motion theory was introduced as a viable simulation method. In the ordinary regime it was shown that use of the conventional step-by-step discrete methods is enormously time-consuming for adequate exploration of the pore space, and a more elegant method based on the first passage time (FPT) distribution for random walkers was introduced. The ordinary regime tortuosities thus calculated were well represented by $\tau = 1/\phi$ at high porosities. Since the FPT method could not be used for $N_{Kn} > 0.5$, the unadorned MSD technique was used for higher Knudsen numbers. In particular, the limits of the transition regime in these media were quantified for the first time, and the Knudsen asymptotic tortuosities agreed with those computed by a different technique. As Kim and Torquato (1990) point out, the largest sources of error are due to the finite number of random walkers used and the finite length of their walks.

The MSD method, especially with the FPT embellishment, appears particularly suited to transition and molecular regime transport calculations in disordered two-phase dispersions of arbitrary inclusion geometry. For instance, a potential application is in measurement of the directional diffusivities in 2-D layered wave preforms, which are also densified using CVI. An examination of Eq. 3 shows that the MSD method can be applied to such anisotropic systems as well, provided the individual displacements are independent of each other. If a small scale representation of the actual medium can be constructed on the computer, the MSD method can be applied with success, even in the transition regime where no model equation presently exists.

Acknowledgment

The authors are grateful to Sebastian C. Reyes of Exxon Research and Engineering for numerous useful discussions concerning his hybrid random walk technique and to Stratis V. Sotirchos for critical examination of our results. This research was supported by the Minnesota Supercomputer Institute and the National Science Foundation.

Notation

$\bar{d}$ = mean pore dimension
D = diffusion coefficient
$E[\cdot]$, $\langle\rangle$ = expectation, mean
e_0, e_2 = errors in 0th, 2nd moments
f = distribution
f_T = transmitted fraction
l_f = fiber length
L = penetration depth
n = number of steps
N = number
N_c = number of cylinders
N_{Kn} = Knudsen number
$P(t,x;r)$ = first passage time (FPT) distribution
r_f = fiber radius
R = radius of imaginary sphere
s = specific surface area
S = displacement
t = time
t_0 = probe time
t' = dimensionless variate from FPT
$\bar{v}$ = mean molecular velocity
V = simulation volume
x, y, z = position coordinates

Greek letters

δ = boundary layer thickness
λ = mean free path
λ_{true} = actual mean free path in porous solid
λ_{free} = free space value
ϕ = porosity
ϕ_c = percolation threshold
σ = standard deviation
τ = tortuosity
ξ = uniform random variate; upper integration limit in Eqs. 29 and 30

Subscripts

cont = continuum
disc = discrete
f = fiber
i = step index
inc = inclusion
Kn = Knudsen
max = maximum
min = minimum
M = molecule
o = origin

Superscripts

A = accessible
eff = effective

Literature Cited

Abbasi, M. H., J. W. Evans, and I. S. Abramson, "Diffusion of Gases in Porous Solids: Monte Carlo Simulations in the Knudsen and Ordinary Diffusion Regimes," *AIChE J.*, **29**, 617 (1983).

Akanni, K. A., J. W. Evans, and I. S. Abramson, "Effective Transport Coefficients in Heterogeneous Media," *Chem. Eng. Sci.*, **42**, 1945 (1987).

Aris, R. *The Mathematical Theory of Diffusion and Reaction in Permeable Catalysts*, Vol. I, Clarendon Press, Oxford, (1975).

Beran, M. J., and N. R. Silnutzer, "Effective Electrical, Thermal and Magnetic Properties of Fiber Reinforced Materials," *J. Compos. Mater.*, **5**, 246 (1971).

Burganos, V. and S. Sotirchos, "Simulation of Knudsen Diffusion in Random Networks of Parallel Pores," *Chem. Eng. Sci.*, **43**, 1685 (1988).

Coleman, R., "Random Paths Through Convex Bodies," *J. Appl. Prob.*, **6**, 430 (1969).

Einstein, A., *Investigations on the Theory of the Brownian Movement*, Dover, New York (1926).

Evans, J.W., M. H. Abbasi, and A. Sarin, "A Monte Carlo Simulation of the Diffusion of Gases in Porous Solids," *J. Chem. Phys.*, **72**, 2967 (1980).

Faley, T. L. and W. Strieder, "The Effect of Random Fiber Orientation on Knudsen Permeabilities," *J. Chem. Phys.*, **89**, 6936 (1988).

Fanti, L. A. and E. D. Glandt, "Particle Trapping in Microporous Media," AIChE Meeting, San Francisco (1989).

Hashin, Z. and S. Shtrikman, "A Variational Approach to the Theory of the Effective Magnetic Permeability of Multiphase Materials," *J. Appl. Phys.*, **33**, 1514 (1962).

Jackson, R., *Transport in Porous Catalysts*, Elsevier, New York, (1977).

Keller, J. B., "Conductivity of a Medium Containing a Dense Array of Perfectly Conducting Spheres or Cylinders or Nonconducting Cylinders," *J. Appl. Phys.*, **34**, 991 (1963).

Kim, I. C., and S. Torquato, "Determination of the Effective Conductivity of Heterogeneous Media by Brownian Motion Simulation," *J. Appl. Phys.*, **68**, 3892 (1990).

Loeb, L. B., *The Kinetic Theory of Gases*, McGraw Hill, New York (1934).

Maxwell, J. C., *A Treatise on Electricity and Magnetism*, **1**, Clarendon, Oxford (1881).

Melkote, R. R., and K. F. Jensen, "Gas Diffusion in Random Fiber Substrates," *AIChE J.*, **35**, 1942 (1989).

Naslain, R., H. Hannache, L. Heraud, J. Rossignol, F. Christin, and C. Bernard, "Chemical Vapor Infiltration Technique," *Proc. Euro. CVD-4*, Eindhoven, 293 (1983).

Perrins, W. T., D. R. McKenzie, and R. C. McPhedran, "Transport Properties of Regular Arrays of Cylinders," *Proc. R. Soc. Lond. A.*, **369**, 207 (1979).

Rayleigh, R. S., "On the Influence of Obstacles Arranged in Rectangular Order upon the Properties of a Medium," *Phil. Mag.*, XXXIV-Fifth Series, 481 (1892).

Reyes, S. and E. Iglesia, "Effective Diffusion Coefficients in Catalyst Pellets: New Model Porous Structures and Transport Simulation Techniques," *J. Catal.*, **129**, 457 (1991).

Sangani, A. S., and C. Yao, "Transport Processes in Random Arrays of Cylinders. I. Thermal Conduction," *Phys. Fluids*, **31**, 2426 (1988).

Satterfield, C. N., *Mass Transfer in Heterogeneous Catalysis*, MIT Press, Cambridge (1970).

Schwartz, L. M., and J. R. Banavar, "Transport Properties of Disordered Continuum Systems," *Phys. Rev. B.*, **39**, 11965 (1989).

Schwartz, L. M., J. R. Banavar, and B. I. Halperin, "Biased-Diffusion Calculations of Electrical Transport in Inhomogeneous Continuum Systems," *Phys. Rev. B.*, **40**, 9155 (1989).

Siegel, R. A. and R. Langer, "A New Monte Carlo Approach to Diffusion in Constricted Porous Geometries," *J. Colloid Inter. Sci.*, **109**, 426 (1986).

Smith, P. A. and S. Torquato, "Computer Simulation Results for Bounds on the Effective Conductivity of Composite Media," *J. Appl. Phys.*, **65**, 893 (1989).

Tassopoulos, M. and D. E. Rosner, "Simulation of Vapor Diffusion in Anisotropic Particulate Deposits," *Chem. Eng. Sci.*, submitted (1991).

Tomadakis, M. and S. Sotirchos, "Knudsen Diffusivities and Properties of Structures of Unidirectional Fibers," *AIChE J.*, **37**, 1175 (1991).

Torquato, S., "Thermal Conductivity of Disordered Heterogeneous Media from the Microstructure," *Rev. Chem. Eng.*, **4**, 151 (1987).

Torquato, S. and J. D. Beasley, "Effective Properties of Fiber-Reinforced Materials: I-Bounds on the Effective Thermal Conductivity of Dispersions of Fully Penetrable Cylinders," *Int. J. Engng. Sci.*, **24**, 415 (1986).

Torquato, S., and I. C. Kim, "Efficient Simulation Technique to Compute Effective Properties of Heterogeneous Media," *Appl. Phys. Lett.*, **55**, 1847 (1989).

Torquato, S., and F. Lado, "Bounds on the Effective Transport and Elastic Properties of a Random Array of Cylindrical Fibers in a Matrix," *J. Appl. Mech.*, **55**, 347 (1988).

Tsai, D. S. and W. Strieder, "Effective Conductivities of Random Fiber Beds," *Chem. Eng. Commun.*, **40**, 207 (1986).

Verlet, L., "Computer 'Experiments' on Classical Fluids I. Thermodynamical Properties of Lennard-Jones Molecules," *Phys. Rev.*, **159**, 98 (1967).

Wakao, N. and J. M. Smith, "Diffusion in Catalyst Pellets," *Chem. Eng. Sci.*, **17**, 825 (1962).

Weiss, G. H., "First Passage Time Problems in Chemical Physics," *Adv. Chem. Phys.*, **13**, 1 (1967).

Weissberg, H. L., "Effective Diffusion Coefficient in Porous Media," *J. Appl. Phys.*, **34**, 2636 (1963).

Manuscript received July 3, 1990, and revision received Oct. 7, 1991.